Dawn-side magnetopause observed by the Equator-s magnetic field experiment: Identification and survey of crossings

M. W. Dunlop[1], A. Balogh[1], W. Baumjohann[2], G. Haerendel[2], K.-H. Fornacon[3] and E. Georgescu[2,4]

[1]Space and Atmospheric Physics Group, Imperial College, London SW7 2BZ, England.

[2]Max-Planck-Institute für extraterrestrische Physik, Garching, Germany.

[3]Institut für Geophysik und Meteorologie, TUB, Braunschweig, Germany.

[4]Institute of Space Sciences, Bucharest, Romania.

Abstract. The German Equator-S spacecraft provided long duration, low latitude coverage of the dawn-side magnetopause and adjacent magnetosheath. We document 131 magnetopause crossings from 31 orbits, giving coverage from 06:00 to 10:40 LT and exhibiting a wide range of local magnetic shear. The Tsyganenko model field is used routinely to assist identification and in categorising the crossings. The apogee of the spacecraft remains close to the magnetopause for mean solar wind pressure. Consequently, magnetosheath intervals often extending several hours are observed, many containing a high number of crossings. For most encounters, a well ordered, tangential (draped) magnetosheath field is observed; 30% containing extended intervals of strong mirror signatures. The occurrence of the crossings is summarised and locations are found to compare well to predicted boundary positions using observed, upstream solar wind IMF and pressure values; some corresponding to unusually high solar wind ram pressure. Other crossing characteristics have also been analysed, such as boundary normals. Although these are broadly consistent with fitted, model magnetopause orientations, they typically lie sun-ward of these, suggesting a blunter magnetopause shape in this region than predicated. No strong evidence is found of large deviations in local boundary orientations, possibly consistent with the highly draped magnetosheath field configuration.

1. Introduction

The Equator-S spacecraft was launched on 2nd December 1997, with subsequent operations providing good coverage of the dawn-side magnetopause and adjacent magnetosheath until the end of March 1998. The spacecraft was placed into an inertial, eccentric, near-equatorial orbit on 11th December 1997, having an apogee height of ~10.6R_E (500x67300km), initially oriented towards ~10:40 LT at the start of science operations (see Figure 2). Other spacecraft have traversed this region, notably ISEE1/2 and AMPTE IRM/UKS, but published data from these missions have often concentrated on the sub-solar region and dusk-side [e.g. *Berchem and Russell*, 1982, *Russell*, 1995, *Paschmann et al.* 1985, 1986, *Phan and Paschmann*, 1995]. Moreover, both the ISEE and AMPTE-IRM/UKS spacecraft had larger apogees, resulting in the fast traversal of the magnetopause region compared to Equator-S. AMPTE/CCE also covered the dawn-side magnetosphere in an orbit similar, to that of Equator-S but with a smaller apogee. As a consequence, the CCE generally remained within the magnetosphere when on the flanks and published crossings of the magnetopause are predominantly limited to the sub-solar region, within an hour of local noon [e.g. *Anderson and Fuselier*, 1993].

By contrast, the Equator-S orbit provided extended coverage down to 06:00 LT of the dawn-side, inner magnetosheath close to the magnetopause during average or compressed magnetospheric conditions (typically corresponding to dynamic pressures of ~1.5-4 nPa). Here, we catalogue all observed traversals across the magnetopause and note the local and solar wind conditions associated with each. Often, the encounters produced a large number of multiple crossings, and extended intervals in the boundary region (a few to several hours on occasions). We identify unusual encounters by virtue of high dynamic pressure or particular magnetosheath characteristics. We also compare the positions of the main crossings to predicted boundary locations. Furthermore, we routinely compare results of boundary normal analysis to expected orientation and to indicate tangential alignment of the magnetic field through the crossings.

2. Magnetopause identification

The data used for this study were taken by the magnetic field experiment (MAM), which provided data from 16th December 1997 onward. The experiment consisted of two pairs of flux-gate magnetometers, positioned on two opposing 1.8m booms, each located at, and 50cm inward, from the boom ends. The instruments measure in four ranges between 250 and 64,000nT at 16 bit digital resolution. At nominal telemetry rate, the instruments are capable of providing high time resolution DC magnetic field data up to 128 Hz, when data from only one magnetometer on the boom are telemetered to ground. Use of both magnetometers reduces the data rate to 64 Hz, but allows cross calibration between the sensors. Since a feature of the mission was operation at a high spin rate, processed, spin averaged data at ~1.5 sec resolution were employed for the current study. (Note that the spin rate was reduced from 50 rpm to about 40 rpm during the mission.)

Although the ion composition data (ICI), and energetic particle data (EPI) were also taken from mid February and mid January, 1998, respectively, at the time of this report MAM is the only calibrated data set available routinely during the whole of this early phase of the mission. All crossings have therefore been identified only by the magnetic field data, but assisted by use of the *Tsyganenko and Usmanov* [1987], *Tsyganenko* [1989] model field. This provides a number of comparative features, as shown by

Figure 1 which illustrates the first magnetopause encounters. Firstly, the model trace provides a background configuration for the magnetospheric field which can better reveal different field orientations in the magnetosheath; at least for high shear events, best identified by sharp changes in field orientation alone. Secondly, it provides a nominal value for the field intensity near the magnetopause with which to compare magnetospheric state.

In the crossings observed here, the magnetospheric field generally lies close to the model field orientation, while the magnetosphere is often in a magnetically compressed state, with a greater than nominal field magnitude at the magnetopause. Discontinuities in the magnetosheath of solar wind origin can usually be distinguished from true magnetopause crossings by comparison to the model field. Only a few low shear crossings were observed and these have been identified more approximately by changes in field magnitude, or an enhancement of magnetic variance. A problem with identification in the absence of a strong discontinuity is the risk of confusion with any boundary layer signature. Typically, the magnetosheath field often exhibited distinctive characteristics, such as mirror mode waves (further analysed in *Lucek et al.* [submitted to GRL]), which differ from those of the magnetosphere and make miss-identification unlikely.

Figure 1 shows the magnetic field orientation and magnitude in GSE co-ordinates for both the measured (dark trace) and T87 model (dashed trace) magnetic field (at K_p=1-/1+). The field orientation is defined by θ, the latitude, and ϕ, defined positive from X_{GSE}. This early event, corresponding to above average solar wind pressures (P_{ram}~2.9 nPa) and southward B_z^{IMF}, shows good agreement with the model field in orientation and only a small difference in magnitudes (the T89 model gives a similar comparison). Most crossings show large field rotations, although a number of partial crossings are apparent (at 17:09, 17:13, 17:37, 17:41 and 17:47 UT).

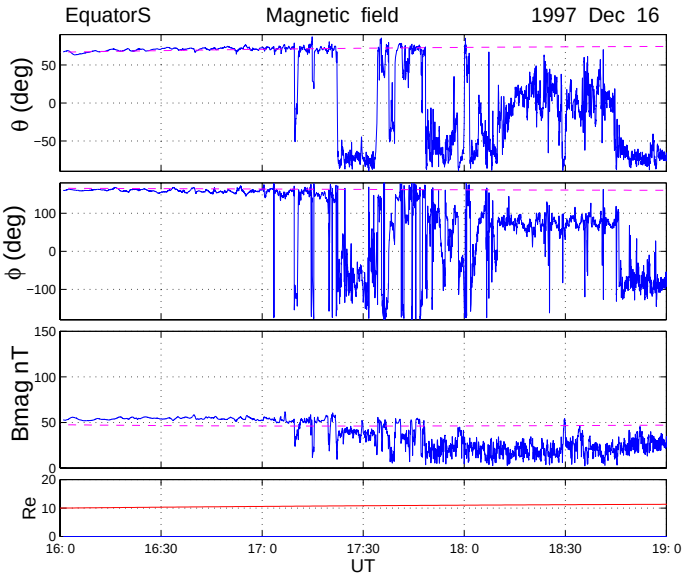

Figure 1. The first observed magnetosheath excursion; given as an example of the identification, using the model field (dashed trace). The magnetic field is expressed in GSE polar co-ordinates.

3. Survey of crossings: occurrence and location

A survey through the complete data set provided by MAM revealed a total of 31 orbits, from 16th December 1997 to 5th March 1998, which each contained at least one clear magnetopause traversal into or out of the magnetosheath. Two further orbits contain signatures which are not clearly magnetopause traversals, since they occurred during a crossing of the dawn-side, tail current sheet, close to 06:00 geographic LT. Figure 2 shows the locations of 131 events, representing complete or partial crossings, projected into the X,Y_{GSE} plane. The corresponding projected spacecraft orbits for each magnetopause pass are also superimposed to indicate occurrence and extent of the coverage achieved. Since the orbit is equatorial, it is inclined in GSE, apogee lying above the plane with all passes having a similar apogee height at ~4.5-4.8R_E. Individual crossings lie at varying heights above the plane in Z_{GSE} (as listed in Table 1), but range only between 2.9-4.8R_E, depending on position around the orbit. Since this represents only a small range of crossing heights, simple projection in X,Y_{GSE} can visually demonstrate crossing locations relative to model boundaries.

Table1: Properties of main magnetopause crossings

Date	UT	LT	z	$(B/B_m)^2$	Kp	P_{ram}	IMF	MP_{shear}	P_{MP}	MSH ordering			#
16/12/97	17 22 00	9:39	3.57	1.44	1	2.9	south	180	-3	Y	sunward	m*	10
18/12/97	14 27 00	9:38	3.61	1.69	0+	2.7	Parker	90	2.3		poor-n		1
19/12/97	14 13 00	9:52	4.02	1.00	1-	1.8	Parker	140	1.8		sunward		5
20/12/97	08 53 00	9:03	2.86	1.96	1	4.5	south	180	-5	Y		m	1
21/12/97	08 31 00	9:19	3.40	1.44	1-	3.3	Parker	170	3	Y	sunward	m	3
22/12/97	06 34 00	9:12	3.30	1.96	1-	4.2	radial	170	3.2			m	6
23/12/97	10 50 00	10:18	4.48	1.00	0+	1.8	Parker	90	-1	Y		m	6
24/12/97	08 04 00	10:02	4.43	1.00	1	1.8	south	170	1.8	Y	poor-n		1
25/12/97	08 26 00	10:23	4.49	1.00	0+	2.2	radial	40	2	Y	sunward		5
28/12/97	05 05 00	10:37	4.33	1.44	0	3.1	Parker	30	3.3	Y	sunward		2
2/1/98	13 06 00	9:08	4.23	1.00	2	1.6	south	130	-1	Y			1
3/1/98	11 36 00	9:07	4.24	1.00	1+	1.3	south	160	-1	Y	sunward		4
4/1/98	10 33 00	9:12	4.40	1.56	1-	2.0	south	80	-1	Y			4
4/1/98	14 14 00	9:55	4.52	1.20	2-	10.8	south	30	-3	Y	sunward		1
6/1/98	04 36 00	8:35	3.41	2.25	4	3.2	perp	130	3	Y	sunward	m	3
6/1/98	05 52 00	8:51	4.19	1.44	4	3.1	south	160	2	Y		m	5
6/1/98	10 24 00	9:43	4.57	2.00	0	2.0	perp	90	2.1		sunward		2
7/1/98	11 32 00	10:22	4.10	4.00	4-	4.9	perp	90	5	Y	sunward		5
8/1/98	08 37 00	9:58	4.31	2.56	2	2.9	north	50	3.2	Y	sunward	m	3
8/1/98	11 03 00	10:43	3.69	5.00	3-	11.5	south	80	11				4
9/1/98	07 30 00	10:05	4.27	1.98	2+	3.1	south	70	-5	Y		m	1
10/1/98	03 35 00	9:30	4.59	1.00	2	2.6	Parker	90	2.2	Y	sunward		5
22/1/98	23 51 00	8:00	4.45	1.00	1	2.6	Parker	170	2.6	Y	sunward		2
23/1/98	03 59 00	8:47	4.66	1.00	1	2.6	Parker	170	2.6	Y			10
24/1/98	21 14 00	8:02	4.57	1.00	2	2.1	radial	120	2	Y	sunward	m	5
30/1/98	14 37 00	8:25	4.67	1.00	4-	3.3	south	180	3	Y	sunward	m	1
1/2/98	05 46 00	7:14	4.28	5.37	3-	8.2	radial	0	+5	Y	sunward	m	2
1/2/98	08 02 00	7:41	4.68	2.83	3-	4.7	radial	30	+5		sunward		2
2/2/98	08 12 00	8:00	4.76	1.73	1	2.0	north	30	+5		sunward		1
5/2/98	22 17 00	7:10	4.44	2.83	1	4.2	Parker	40	4.2	Y	sunward		3
7/2/98	19 15 00	7:09	4.61	3.00	1	4.0	Parker	100	4	Y	sunward		5
7/2/98	21 25 00	7:34	4.78	1.73	1	3.1	Parker	110	3	Y	sunward	m	5
8/2/98	18 06 00	7:12	4.64	2.83	1+	3.9	Parker	180	4	Y	sunward		4
11/2/98	13 09 00	7:03	4.71	1.73	3+	3.7	south	160	3.7		sunward		6
11/2/98	17 01 00	7:53	4.64	3.00	4+	4.5	radial	160	4.3	Y			1
18/2/98	02 08 00	6:52	4.82	5.37	7-	6.3	south	100	4.5	Y	sunward		4
18/2/98	04 53 00	7:27	4.70	2.20	5+	3.1	Parker	50	4.5		sunward		1
5/3/98	21 58 00	6:07	4.92	8.00	4-	7.9	Parker	0	8	Y	sunward	m	1

The majority of crossings lie earthward of the model magnetopause of *Formisano et al.* [1979a], shown in Figure 2, with the bow shock [*Formisano*, 1979b] shown as a cut at Z_{GSE}=4R_E, for guidance. There are clearly three or four active periods where the magnetosheath is sampled on consecutive passes, in between more quiet times where no crossings were observed. Although motional analysis of the magnetopause can not be performed at this stage, it is likely that crossings at the extremes of the magnetosheath intervals correspond most closely to final boundary positions for ambient conditions. Fewer crossings are sampled for the later passes and, correspondingly, crossing locations become more limited to apogee, which is likely to indicate only shallow entries

into the magnetosheath (unless associated with variable, external conditions). It is clear, therefore, that orbital extent limits the observations to mean solar wind conditions at ~10:40 LT and to increasing solar wind dynamic pressure, typically, for the later crossings, as we confirm below.

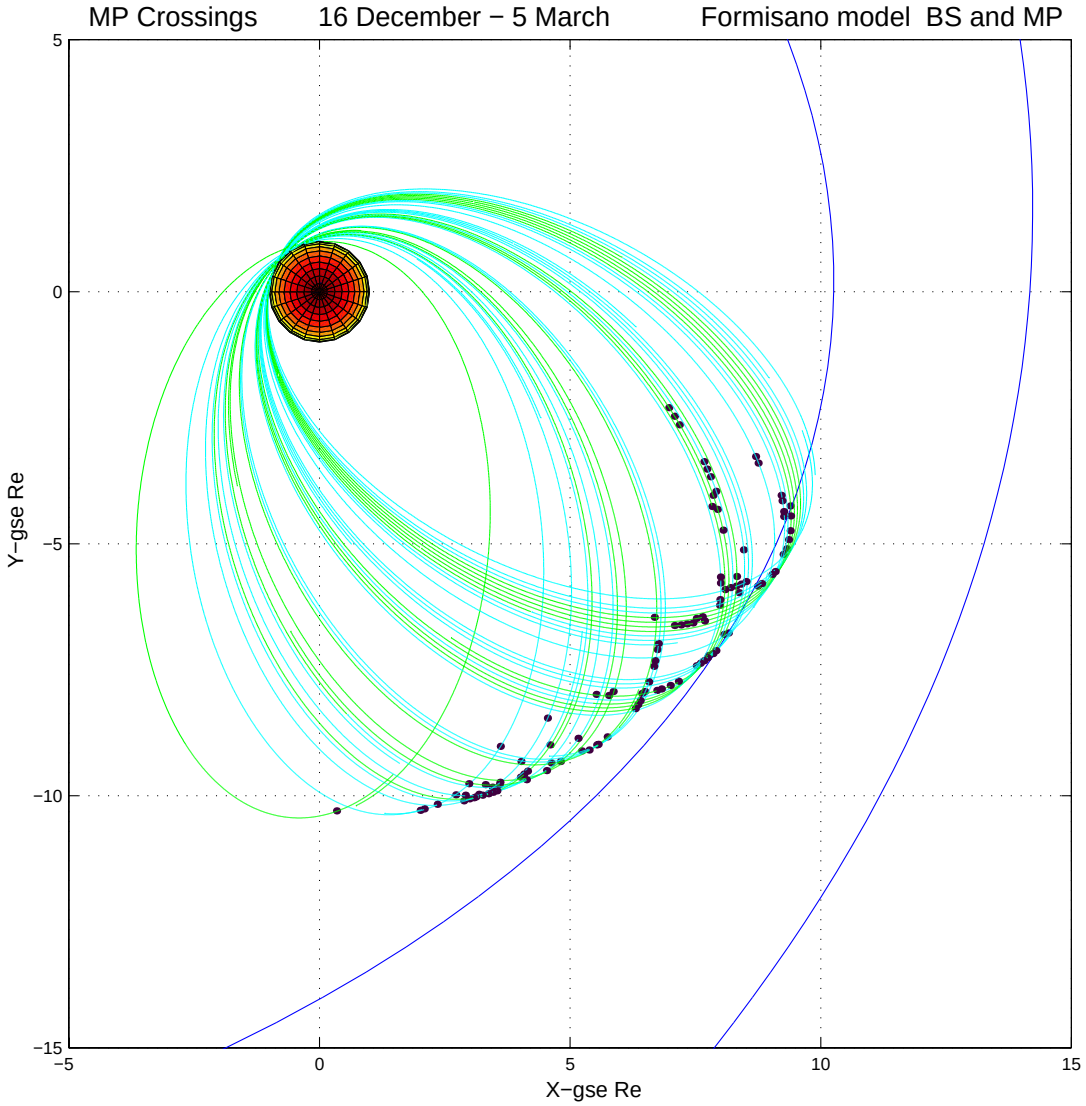

Figure 2. An overview of the crossing locations (scatter points). Equator-S orbits for each of the 31 passes corresponding to the observations (thin, solid traces) are superimposed to better indicate occurrence. The model bow shock and magnetopause for mean solar wind conditions are also shown.

3.1. Categorisation with solar wind and local conditions

Table 1 summarises the occurrence and basic properties of the main crossings for each pass, where we have chosen to list only the final complete crossing. A number of passes, showing extended periods in the magnetosheath (of a few to several hours), have been indicated by two key crossings and the longest excursion into the magnetosheath (6th January) lists three main crossings. The last column in the table shows the number of crossings associated with each main crossing listed. On many of the passes shown in Table 1, the data contain several crossings, consistent either with apogee lying close to the mean magnetopause location, or large amplitude magnetopause motion.

The first columns in the table show date and times, geographic LT and Z_{GSE}, followed by the ratio of observed to model magnetic pressure at the magnetopause. This ratio gives an indication of how locally compressed the magnetosphere is at the time of the crossing, and K_P is also listed to indicate a possibly poor model field comparison. In fact, only a few events occurred during periods of extreme activity ($>K_p$=5), although several show intermediate levels. Solar wind key parameter data, at one hour resolution, obtained predominantly from the WIND spacecraft [*Acuna, et al.*, 1995, and see references in *Russell*, 1995b], have been used to compute the solar wind dynamic pressure from the plasma density and bulk velocity, and to estimate the likely direction of the IMF at the crossing times. The IMF direction is listed to indicate southward or northward B_Z, where this is clear in the WIND data. Otherwise (true for the majority of crossings) alignment along the Parker spiral, radial fields, or orientation perpendicular to the dawn-side bow shock is indicated. At ~200R_E from the Earth, WIND may not identify individual, small scale solar wind features reaching the dawn-side magnetosheath, but should reliably record average conditions, adequate for the purpose here.

Nevertheless, under the column heading MP_{shear} we have also indicated the local magnetic shear angle (degrees) between the magnetospheric and magnetosheath fields. This isn't unambiguous either in identifying sub-solar conditions and the likely magnetopause response, particularly for the dawn-side crossings.

It is clear, however, that an equal number of high and low shear angles (the mean shear angle is ~100º) occur throughout the crossing set and there is no bias to high shear crossings in the data set. Many of the crossings which do not correspond to clear IMF north/south directions do show high local shear, but we choose to address the discussion below to the character indicated by the IMF, primarily, rather than to local shear, initially. This preserves clarity during comparison to the model magnetopause surface used [*Sibeck et al.* 1991], which is parametrised with respect to solar wind IMF and ram pressure values.

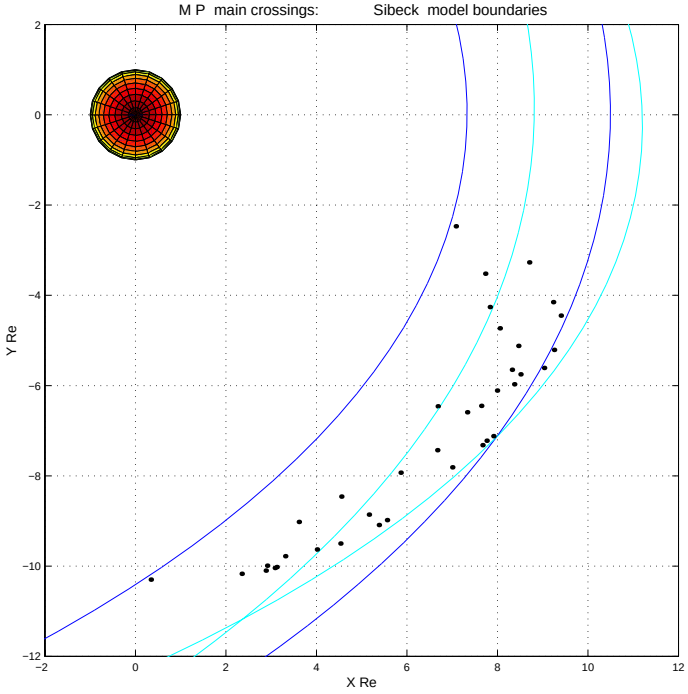

Figure 3. The key crossings for each traversal into or out of the magnetosphere compared to plots of the Sibeck magnetopause model for the range of solar wind dynamic pressures observed (1.8-11 nPa), drawn as thick curves representing cuts through the magnetopause surface at Z=4 R_E. The thin curves represent extremes of IMF-B_Z orientation.

The remaining columns summarise the routine analysis categorising the set of crossings. Firstly, the column headed P_{MP} lists the predicted solar wind conditions required to fit a model magnetopause to the observed crossing positions. Anticipating that the majority of events result predominantly from changing solar wind ram pressure, we indicate the dynamic pressure (written as unsigned numeric values in nPa) required to scale the default pressure surface of *Sibeck et al.* [1991] to crossing position, noting the close agreement to observed values of P_{ram} for the majority of the crossings. For these events, the IMF showed no clear north/south orientation, suggesting simple pressure scaling of position occurs and that use of the simple pressure dependant model surface is valid. The values therefore show that these crossings are consistent with simple pressure balance response. Figure 3 shows the crossings in the table in relation to the *Sibeck et al.* [1991] model, where the dark curves are cuts for the range of pressures found (1.8-11 nPa).

Most of the other crossings occurred during low to medium observed dynamic pressure conditions and were located closer to the Earth than implied by their P_{ram} values. This group were found to uniquely fit a magnetopause shape corresponding to a range of southward orientations of the IMF, consistent with the value of B_Z taken from the WIND observations. Under column P_{MP}, these cases, and those remaining which occurred during northward-IMF, are indicated by signed numeric values (representing field components from -5 to +5 nT) which correspond to the bins of *Sibeck et al.* [1991]. Magnetopause cuts for extreme values of northward and southward IMF are represented by the light curves in Figure 3: the inner, blunt curve represents a southward IMF component of -5 nT, the outer represents the +5 nT surface. These curves are shown to illustrate, at least for this data set, that comparison between solar wind pressure and IMF effects can be uniquely made, since only southward IMF conditions produce closer than expected boundary positions for mean pressure values; except far into the flanks, and these are the crossings we seek to fit. One of the few remaining passes, which was located closer to the earth than implied by the low observed P_{ram} (on the 2nd February, at 8:00 LT), was in fact closely fitted by an extremely northward IMF bin, consistent with the observed value of B_Z (and in fact confirmed by the local magnetic shear angle). Nevertheless, most crossings further into the dawn-side are well (and uniquely) represented by observed, and increasing, dynamic pressure values.

Two passes did correspond to conditions of both medium to high P_{ram} and strongly southward IMF (20th December and the later crossing on 4th January), but did not scale with pressure. They therefore may correspond to particularly unstable conditions, born out by a contrastingly low value of local magnetic compression. A similar argument can be made for the remaining high pressure pass (1st February), which also did not scale with its observed P_{ram}, but then at ~7:30 LT and with no clear IMF-B_Z direction observed (although the local shear confirms northward conditions). Moreover, fitting to B_Z bins is not clear (it is near the cross over in the light curves in Figure 2).

Although the above discussion can be confirmed by inspection of Table 1 and reference to Figure 3, Figure 4 (a) plots P_{ram} against the fitted pressures (P_{MP}) for all these events. It is also instructive, however, to view the trend of the observed P_{ram} and the fitted P_{MP} against $(B/B_m)^2$. These values are plotted in the other panels in Figure 4. In Figure 4(b), the plot of P_{ram} against $(B/B_m)^2$ shows two very high values of P_{ram} out of trend: the first corresponds to the high pressure crossing on the 4th January, mentioned above, and the second to 8th January, which is well fitted by its P_{ram} value. Both occurred during southward conditions, however, so that significant erosion at the magnetopause during these events may account for the low apparent magnetic compression. Other than these crossings, the clearly increasing trend of both parameters supports the view that the majority of events correspond to stable magnetopause position, where the local magnetic compression approximately reflects the ambient measured ram pressure. It is therefore likely that most excursions into the magnetosheath remain close to the magnetopause and any boundary layer. Figure 4(c) in fact shows both the fitted P_{MP} values and the negative (southward IMF) bins and supports the correspondence of magnetopause distance (directly related to P_{MP}) to observed solar wind pressure values. The B_Z values also show that all events occurring under conditions of southward IMF have low magnetic compression ratios, consistent with erosion.

3.2. Boundary analysis and magnetosheath properties

The remaining columns in Table 1, headed 'MSH ordering', give indications of the character of each traversal into the magnetosheath, based on boundary normal analysis which has been routinely carried out on all passes. Boundary normals have been estimated by minimum variance analysis [*Sonnerup and Cahill*, 1967] (MVA) and are compared to the model normals for the fitted surface at each crossing location. The analysis indicates that the

magnetosheath field is predominantly well ordered tangentially to the boundary orientation for most passes, suggesting a well ordered, draped, gross field configuration.

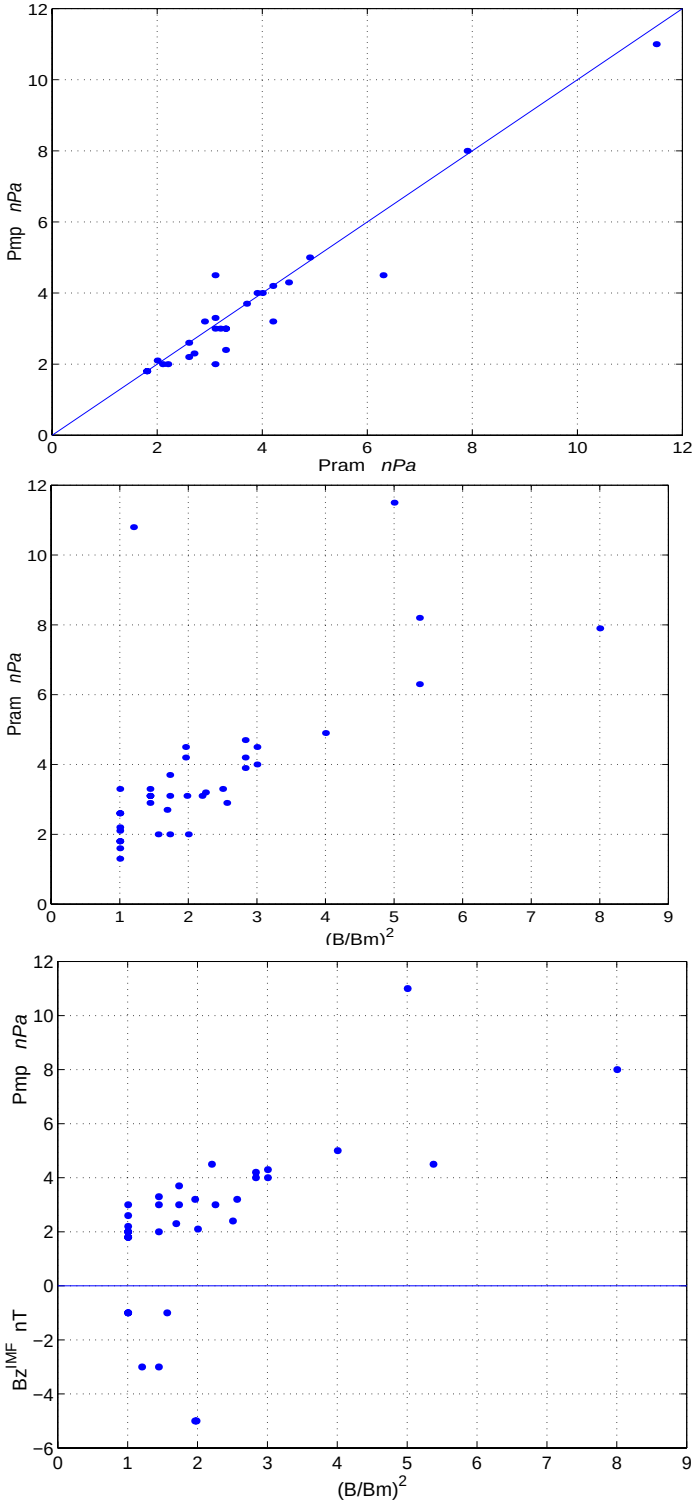

Figure 4. (a) Correspondence between the measured P_{ram} and fitted pressure values (P_{MP}) for crossings occurring during conditions with no B_Z^{IMF}, (b) Correspondence between $(B/B_m)^2$ and P_{ram} for all the key crossings, (c) Correspondence between $(B/B_m)^2$ and crossings fitted to P_{MP} and B_Z^{IMF}.

The first column under 'MSH ordering' indicates when this ordering extends over the whole interval (by 'Y'); identified by only small (<10º) deviations in the mean angle of the magnetic field to the minimum variance direction. Since, particularly on the dawn-side, the expectation is that the magnetosheath field will deviate from that at the boundary [e.g. *Spreiter et al.*, 1966], this again suggests that most magnetosheath excursions are shallow and that the spacecraft typically remains close to the magnetopause. Most of the calculated normals deviate somewhat from the model normals, lying sun-ward of the model orientation in nearly all cases. The second column indicates when the calculated normals differ by a little more than 20° in orientation. This occurs for the majority of the passes, although in context, the variation over the whole set of crossings is as expected, approximately following the model boundary surface orientation, which changes over the range of crossings by more than 60°. It is worth noting here that for the range of local time covered, the difference in local orientation between the fitted magnetopause pressure curves and the curve for the extreme southward bin is never more than a few degrees (as is apparent in Figure 3).

Thus, the model suggests that the effects of erosion on magnetopause shape are insufficient to explain the orientations here and in fact the local magnetic shear appears to show low values as often as high which are not well correlated with the deviation of the MVA normals. It is relevant to note, therefore, that this result for the orientation of the boundary is in contrast to the close agreement found between crossing location and pressure scaling of the model boundary for observed solar wind ram pressure (as well as in relation to the dependence of the model boundary for observed B_Z^{IMF} at low ram pressure). This gives some weight to the conclusion that the measured normals consistently suggest a more flared, or blunter, shape to the magnetopause than indicated by the *Sibeck et al.* [1991] model, rather than arising from poor knowledge of magnetospheric state, poor identification, or other errors.

Although detailed analysis has not been completed, most boundary normals within a pass show very little variation from each other and depend predominantly only on location (LT). Furthermore, where multiple crossings are observed, particularly for the long events, there is, rather unexpectedly, no strong evidence of large local changes in boundary orientation which would be consistent with boundary waves or pressure ripples. This latter result is also consistent with the view that the majority of the crossings arise predominantly from small fluctuations of the magnetopause close to the spacecraft, rather than large amplitude changes from far away. This result may also be a consequence of the strong presence of magnetosheath draping in most intervals of sheath data and ordered, compressional signatures in many of the long intervals. Further work is needed to clarify this.

The third column under 'MSH ordering' indicates when the magnetosheath field contained strong, mirror-like, compressional signatures, over part or all of the interval. These occurred for 30% of the passes and often were of extended duration (hours). All but one correspond to the well ordered (draped) magnetosheath intervals and most begin immediately adjacent to the magnetopause crossing. Of particular note are the two innermost crossings (see Figure 3), for which the solar wind pressure was highest (8th January and 5th March) and which both exhibited high magnetic compression at the magnetopause, at high and low magnetic shear, respectively. Although separated by ~5 hrs LT, both show intense, short intervals of mirror signatures and both are associated with density spikes in the WIND data.

4. Discussion and Conclusions

We have used magnetic field data alone to identify and categorise 131 crossings of the dawn-side magnetopause on 31

orbits, providing long duration coverage of the magnetosheath adjacent to the magnetopause from 06:07 to 10:43 LT. Such extensive coverage in this region is uncommon. The effect of orbital extent is increasingly biased to local conditions associated with intermediate, rather than low, solar wind dynamic pressure, further into the flank region. All crossings have been analysed for their boundary characteristics together with some details of their boundary and near magnetosheath properties. The occurrence of the magnetopause encounters are found to compare well to predicted boundary location, where solar wind conditions (of P_{ram} and B_z^{IMF}) are known, accounting to a large degree for variation in magnetopause location. Magnetopause orientation, however, although broadly consistent with predicted boundary normals, is typically sun-ward of these, implying that the dayside magnetopause is blunter than that predicated by the *Sibeck et al.* [1991] model for the known IMF orientations. It is also possible, however, that this result implies that a simple magnetopause shape is not entirely sufficient to describe magnetopause orientation in this region. The presence of high local magnetic shear at the magnetopause in general does not occur sufficiently regularly to explain this result. Most events yield stable normals and exhibit good tangential ordering of the magnetosheath field throughout the intervals, consistent with strong draping and/or proximity to the magnetopause, with only a few exceptions.

A discussion of individual passes and the detailed analysis of their characteristics is beyond the scope of this first report. It is appropriate, however, to indicate the presence of key phenomena, as in the previous section. A number of intervals of a few to several hours, and containing a high number of repeated crossings, were observed, providing extended coverage of the near-magnetosheath. A few encounters exhibiting unusually high magnetic pressure states were also found. Of particular note are the occurrence of strong mirror-like signatures in the adjacent magnetosheath during a significant fraction (~30%) of the encounters for extended periods.

Although not explicitly shown here, the field models generally match the set of events more poorly than that shown in Figure 1, worsening with decreasing local time. Typically, the T87 model fits the data no worse than the T89 model during conditions of low to intermediate K_P index near the magnetopause, and is often better for passes located further into the flank region. Near the dawn-side tail current sheet, typically, T87 also fits better (then at high P_{ram}), which is thought to be a result of the form of the tail current sheet used in T89. We hope to extend this study with plasma data, where available, in order to analyse MP motion and pressure balance, for example.

Acknowledgement. The Equator-S mission was made possible through grant 500C94024 by the German Space Agency (DARA/DLR).

References

Acuna, M, K. W. Ogilvie, D. N. Baker, S. A. Curtis, D. H. Fairfield, and W. H. Mish, The global Geospace program and its investigations, *Space Sci. Rev.*, **71**, 5, 1995.

Anderson, B. J. and S. A. Fuselier, Magnetic pulsations from 0.1 to 4.0 Hz and associated plasma properties in the Earth's subsolar magnetosheath and plasma depletion layer, *J. Geophys. Res.*, **98**, 1461-1479, 1993.

Berchem, J. and C. T. Russell, The thickness of the magnetopause current layer: ISEE 1 and 2 observations, *J. Geophys. Res.*, **87**, 2108-2114, 1982.

Formisano V., V. Domingo, and K.-P. Wenzel, The three dimensional shape of the magnetopause, *Planet. Space Sci.*, **27**, 1137-1149, 1979a.

Formisano V., Orientation and shape of the Earth's bow shock in three dimensions, *Planet. Space Sci.*, **27**, 1151-1161, 1979b.

Phan, T. -D. and G. Paschmann, The magnetosheath region adjacent to the dayside magnetopause, *in Physics of the Magnetopause, Song, Sonnerup and Thompsen (eds)*, AGU Geophysical Monograph **90**, 115-122, 1995.

Paschmann, G., I. Papamastorakis, W. Baumjohann, N. Skopke, C. W. Carlson, B. U. Ö. Sonnerup, and H. Lühr, ISEE observations of the magnetopause: Reconnection and the energy balance, *J. Geophys. Res.*, **90**, 12111-12120, 1985.

Paschmann, G., I. Papamastorakis, W. Baumjohann, N. Skopke, C. W. Carlson, B. U. Ö. Sonnerup, and H. Lühr, The Magnetopause for large magnetic shear: AMPTE/IRM observations, *J. Geophys. Res.*, **91**, 11099-11115, 1986.

Russell, C. T., The structure of the magnetopause, *in Physics of the Magnetopause, Song, Sonnerup and Thompsen (eds)*, AGU Geophysical Monograph **90**, 81-98, 1995.

Russell, C. T. *(ed)*, The Global Geospace Mission, *Space Science Rev.*, Kluwer Academic Publications, **71**, 1995b.

Sibeck, D. G., R. E. Lopez, and E. C. Roelof, Solar wind control of the magnetopause shape location and motion, *J. Geophys. Res.*, **96**, 5489, 1991.

Sonnerup, B. U. O. and L. J. Cahill, Magnetopause structure and attitude from Explorer 12 observations, *J. Geophys. Res.*, **72**, 171-183, 1967.

Spreiter, J. R., A. L. Summers, and Y. Alksne, Hydromagnetic flow around the magnetosphere, *Planet. Space Sci*, **14**, 223-253, 1966.

Tsyganenko N. A. and A. V. Usmanov, Global quantitative models of the geomagnetic field in the cislunar magnetosphere for different disturbance levels, *Planet Space Sci*, **35**, 11, 1347-1358, 1987.

Tsyganenko N. A., A magnetospheric field model with a warped tail current sheet, *Planet. Space Sci.*, **37**, 1, 5-20, 1989.

M. W. Dunlop, Space and Atmospheric Physics Group, Blackett laboratory, Imperial College of Science Technology and Medicine, London, SW7 2BZ, UK. (m.dunlop@ic.ac.uk)

(Received; revised; accepted.)

Paper number.

Index Terms

2724 Magnetopause, cusp, and boundary layers
2728 Magnetosheath
2740 Magnetospheric configuration and dynamics